RSC Advances

PAPER

Cite this: *RSC Adv.*, 2022, **12**, 11047

Co-ligand triphenylphosphine/alkynyl-stabilized undecagold nanocluster with a capped crown structure†

Yan-Li Gao, * Shiqing Bi, Yufei Wang, Jian Li, Ting Su and Xuchun Gao

Received 18th February 2022
Accepted 4th April 2022

DOI: 10.1039/d2ra01080a

rsc.li/rsc-advances

We report the synthesis and crystal structure of novel co-ligand phosphine/alkynyl protected Au nanoclusters, with composition $[Au_{11}(PPh_3)_8(C{\equiv}CPh{-}CF_3)_2](SbF_6)$ (1). The gold atoms in the cluster as a capped crown structure subtend C_{3v} symmetry with one deriving from a central icosahedron and 10 peripheral Au atoms, and all alkynides are exclusively σ coordination bonding. The mean core diameter is about 5.1 Å and the overall van der Waals diameter can be estimated to be 20.5 Å. The optical absorbance of 1 in solution reveals characteristic peaks at 384 and 426 nm and a shoulder between 450 and 550 nm.

Introduction

Metal clusters are deemed as ideal miniatures of organic-capped metal nanoparticles due to their intermediate size regime that bridges the molecules and plasmonic nanoparticles.[1–4] Gold nanoclusters have attracted increasing attention owing to their potential applications in luminescence, catalysis, sensing, and biology.[5–11] Ligand-protected gold nanoclusters having well-defined compositions and structures are of great significance in terms of the correlation of structures and properties.[12–14] During the past decades, great progress has been made in engineering interfaces of metal nanomaterials *via* single ligand systems, for instance, phosphine, thiol, alkynyl, halide, and *N*-heterocylic carbene,[15–22] which readily promote the surface reactivity of nanoclusters, thereby helping to achieve high catalysis performance.[23]

The pioneering work of ($[Au_{11}(PPh_3)_7](SCN)_3$) can be traced back to Malatesta *et al.* in 1966, but the structure could not be accurately defined at that time.[24,25] Subsequently, a series of smaller phosphine-capped gold clusters with nuclearity of 5–13 were synthesized and structurally characterized.[26,27] Mingos *et al.* then predicted the complete icosahedral Au13 structure and later achieved it experimentally.[28] Thereafter, major interests in ligand-coordinated gold clusters moved to heterometallic, higher-nuclearity, and thiolate-capped families.[29–32] Schmid *et al.* reported the Au55 cluster, but its insufficient solubility precluded crystallization and mass spectrometry confirmation of the $Au_{55}(PPh_3)_{12}C_{l6}$ formula, but no crystal structure has been attained to date.[33]

In addition to the habitual thiolate and phosphine ligands, alkynyl-protected nanoclusters often exhibit highly regular structures and typical coordination motifs forming fascinating assemblies exploiting this versatile coordination.[34–39] Metallophilic interactions are often an important driving force for the formation of large clusters. Their structural features were exemplified in a series nanoclusters and intermetallic with interesting alkynyl-Au staple motifs,[40–44] which resemble thiolate-protected Au nanoclusters.[45–51] Gold complexes exhibit very simple coordination modes of the alkynyl ligands, dominated by two, the simple μ_2-η^1 end-on and the bridging μ_2-$\eta^1\eta^2$ mode. That means the bonding of alkynyl ligands with golds can form σ coordination bond as well as π coordination bond, which is unlike thiol ligands, resulting the coordination mode very rich.

Recently, co-ligands have been used to endow metal nanomaterials with better performance than either of single ligand systems. However, in sharp contrast to the well-studied pure-ligand–metal interface, it remains an unsettled front for today's characterization techniques to fully identify the detailed binding structures in mixed-ligand metal nanomaterial systems, as they often lead to highly complicated surface structures or dynamic ligand arrangements.[52–54]

Herein, we report the preparation and structure determination of hybrid ligands protected gold nanocluster with the composition of $[Au_{11}(PPh_3)_8(C{\equiv}CPh{-}CF_3)_2](SbF_6)$ (**1**). The Au-skeleton have C_{3v} symmetry of icosahedron that have one centered and 10 peripheral Au atoms. It is present in the conventional $Au_{11}(PAr_3)$ clusters for various combinations of phosphine, sub-ligands and counter anion.[55,56] And unlike in the other gold system for this undecagold cluster all alkynides are exclusively in their μ_1-η1-end-on coordination mode.

School of Chemistry and Chemical Engineering, Yulin University, Yulin 719000, China. E-mail: gaoyanli8503@126.com

† Electronic supplementary information (ESI) available: The experimental section, structure information in detail and additional NMR data. CCDC 2127378. For ESI and crystallographic data in CIF or other electronic format see https://doi.org/10.1039/d2ra01080a

Result and discussion

The undecagold cluster $[Au_{11}(PPh_3)_8(C{\equiv}CPh{-}CF_3)_2](SbF_6)$ was synthesized by $NaBH_4$ reduction of PPh_3AuCl and $RC{\equiv}CAu$ with SbF_6 anion in methanol. After reduction and centrifugation, the dark brown residue was dried up to afford brown solid. Further crystallization from dichloromethane/hexane led to the formation of black rod-shaped crystals.

The single-crystal X-ray analysis revealed that $[Au_{11}(PPh_3)_8(C{\equiv}CPh\text{-}CF_3)_2](SbF_6)$ crystallizes in the triclinic space group *P*-1 with two formula units (Table S1†). The unit cell parameters as follows: a = 16.0672 Å, b = 17.0707 Å, c = 32.9552 Å; α = 80.8164°, β = 82.7276°, γ = 63.1499°. The packing structure of **1** is shown in Fig. S1† with two molecules in one unit cell. The molecular structure of **1** is shown in Fig. 1 comprising eleven Au atoms, eight PPh_3 and two $RC{\equiv}C$ ligands, and one SbF_6^- anion. The structure of the coordination polyhedron formed by the Au atoms possesses the local symmetry C_3 (3) and approximately C_{3v} (3m) derived from a centered icosahedron.[57,58] This geometry can also be viewed as a capped crown,[59] which is also found for Au_{10} clusters.[60] The Au_{11} core has one central and ten peripheral Au atoms. The Au_{11} core units can be described as capped chairs (icosahedron derivatives). Eight surface Au atoms are coordinated by triphenylphosphine ligand and the other two Au atoms bind to alkynyl ligand. The alkynyl ligands coordinate with Au atoms are in the μ_1-η1-end-on coordination mode, which is unlike in most undecagold species (μ_2-η1η2 mode).

The gold cluster core geometry is similar to the one found in $Au_{11}(PAr_3)_7X_3$ (X = halide or pseudohalide). The structure is compared to $[Au_{11}(PPh_3)_7Cl_3]$(**2**).[58] The substitution pattern of the bulky alkynyl groups and the small halides is different, which has an influence on the Au–Au bond lengths and angles. As observed for most centered Au clusters, the radial Au–Au bond lengths of [2.6273(8)–2.7279(7) Å] in **1** but [2.6079(7)–2.7044(7) Å] in **2**, are significantly shorter than the peripheral bond lengths [2.8062(8)–3.3125(9) Å] (Table S2†), which is [2.84504(7)–2.9677(7) Å] in **2**. The center-to-peripheral radial bond distances are shorter than the peripheral bond distances, indicating the crucial contribution of radial bonding to the stability of cluster skeleton, as observed before. Its mean bond length of 2.7934 Å. The minimal length of 2.6273(8) Å is short for gold clusters while the maximal length of 3.3125(11) Å is quite large.

The mean core diameter is about 5.1 Å (minimal 4.7 Å, maximal 5.4 Å), which was measured between the centers of the Au atoms of opposite sides of the cluster. And the overall van der Waals diameter could be estimated to 20.5 Å which is deduced from measuring the distance between the hydrogen atoms at opposite sides of the cluster (center to center) and the addition of 2.5 Å for the van der Waals radii of the hydrogen atoms. They are all bigger than cluster **2**, which respectively is 4.9 Å, 4.7 Å and 5.3 Å.

In addition, the length of the Au–P bond are from 2.271(3) to 2.305(3) Å in ungecaglod cluster and the mean bond length is 2.287 Å, while the Au–C bond lengths are 1.982(15) Å and 2.026(18) Å respectively. These are in good agreement with those gold clusters in general. The coordination geometries of Au(core)–Au–L (L = P, C) are almost linear, that the angles are from 170.7(1)° to 178.9(5)°. The angle of Au(4)–Au(1)–Au(7) is 125.02(3)° (The Au atom refers to the atom that connected to the alkynyl group, Table S2†).

The sample was further characterized by a ESI-MS spectrometer with an electrospray ionization source under positive mode in CH_2Cl_2 (Fig. 2). The spectrum is quite clean, with the molecular ion peak $[Au_{11}(PPh_3)_8(C{\equiv}CPh{-}CF_3)_2]^+$ at m/z = 4602.4 being dominant. Perfect agreement was observed between the experimental spectrum and simulated isotopic distribution pattern. 8 of the 11 gold atoms should have a valence of zero in order to fulfill the requirement of charge balance. According to the superatom theory, 8 electrons available for cluster bonding a shell closing within the jellium model is plausible (1s and 2p state), leading to an electronically stable compound, which is corresponding to mass spectrum.

The optical absorbance of the dilute solution is easily to obtain and provides first information on the quality of product. Specifically, the size dispersity of the nanoparticles plays a significant role, because the spectrum of molecular clusters

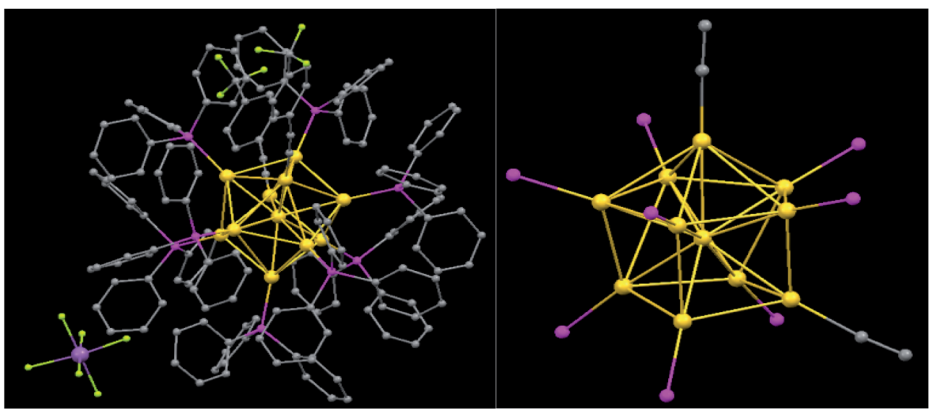

Fig. 1 Molecular view of $[Au_{11}(PPh_3)_8(C{\equiv}CPh{-}CF_3)_2](SbF_6)$ (left) and central cores of triphenylphosphine/alkynyl-stabilized undecagold (right). Color codes for atoms: yellow spheres, Au; pink spheres, P; green spheres, F; grey spheres, C. All hydrogen atoms are omitted for clarity.

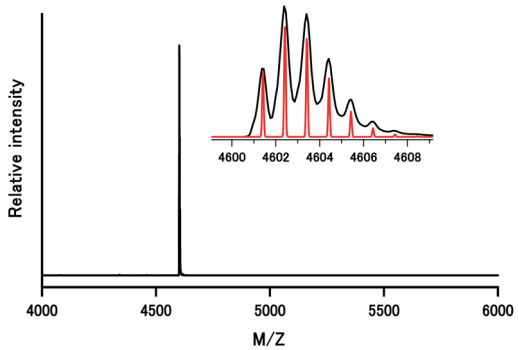

Fig. 2 ESI-MS spectrum of **1** crystals dissolved in CH_2Cl_2. Inset: the experimental (black trace) and simulated (red trace) isotopic patterns of molecular ion peak.

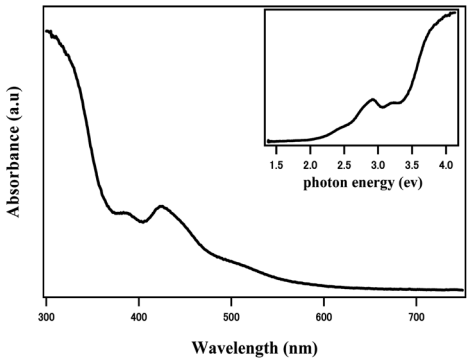

Fig. 3 UV/Vis absorbance spectra of **1** in CH_2Cl_2. Peaks at 384 and 426 nm and a shoulder between 450 and 550 nm confirm the molecular character. Inset: spectrum with a photon energy scale.

shows obvious characteristics, which are sensitive to the number of metal atoms, charge and conformation of the core, whereas the spectrum of metallic colloids (>2 nm) possesses feature and broad inter band and plasmon bands. Fig. 3 presents the UV-vis absorption spectrum of **1** in CH_2Cl_2. The spectrum exhibits an intense absorption band at 426 nm which corresponds to water-soluble undecagold and characteristic of phosphine-stabilized undecagold. Apart from the 426 nm band, there are an intense absorption at 384 nm and a broad absorption of the peak between 450 and 550 nm. This absorption feature at 384 nm should arise from the $[Au_{11}(PPh_3)_8(-C{\equiv}CPh{-}CF_3)_2]^+$ cation, as revealed in the crystal structureFig. 3.

The NMR spectrum recorded in $CDCl_3$ revealed both only one singlet at $\delta = 63.29$ ppm for ^{19}F and 52.32 ppm for $^{31}P\{^1H\}$ Fig. 4, although discrimination between three chemically in equivalent positions of phosphorus atoms is possible in the solid structure of **1**. The observation of only one singlet show that the cluster is dynamic in solution as frequently observed in cluster science, leading to a lower number of signals than expected from the solid-state structure.[5]

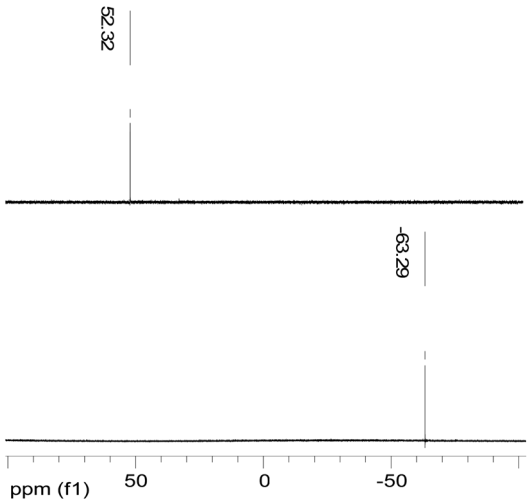

Fig. 4 $^{31}P\{^1H\}$ (top) and ^{19}F (bottom) NMR of **1** in $CDCl_3$ at room temperature.

Experimental

All reagents were obtained from commercial sources and used without further purification.

Synthesis of $[Au_{11}(PPh_3)_8(C{\equiv}CPh{-}CF_3)_2](SbF_6)$ (1)

In a typical synthesis, 7.4 mg (0.015 mmol) of PPh_3AuCl and 1.8 mg (0.005 mmol) of CF_3–PhC≡CAu were dissolved in 3 mL toluene. To the solution 5 mg $NaSbF_6$ in 0.5 mL ethanol was added. The solution was stirred for 10 min. After that, a freshly-prepared NaBH4 solution in methanol (1 mg mL^{-1}) was dropwise added. The solution turns from pale brown to finally dark brown. The reaction continued for 24 h in the dark. It was centrifuged for 2 min at 14 000 rpm. The solution was then dried up to afford brown solid. The solid was thoroughly washed with hexane and ether. 2 mL of dichloromethane was finally used to dissolve the raw product. After filtering, the solution was subjected to the diffusion of hexane in the dark. Black rod crystals were obtained after 4 weeks in a yield of ~36.2% (based on Au).

General characterizations

UV-vis spectra were collected by Shimadzu UV-2550 Spectrophotometer. Mass spectra were recorded on an Agilent Technologies ESI-TOF-MS. Thin-layer chromatography (TLC) was carried out with silicycle pre-coated silica gel plates. NMR spectra were recorded at room temperature on a Bruker AV-500 spectrometer in chloroform-d3 with TMS and chloroform signal as an internal reference.

Crystal structure determinations

The X-ray diffraction intensities were collected for selected single crystals nanocluster $[Au_{11}(PPh_3)_8(C{\equiv}CPh{-}CF_3)_2](SbF_6)$ using an Agilent Technologies SuperNova system. X-ray single-crystal diffractometer using Cu Kα ($\lambda = 1.54184$ Å) at 100 K. The data were processed using CrysAlisPro.[61] The structure was solved and refined using Full-matrix least-squares based on F^2

using ShelXT,[62] ShelXL[63] in Olex2 (ref. 64) and Shelxle.[65] Almost all hydrogen atoms were located from difference Fourier maps and those not found were added at theoretical positions using the riding model. Further details can be obtained from the cif files deposited at the Cambridge Crystallographic Data Centre. The CCDC reference number is 2127378. The thermal elipsoids of the ORTEP diagram at 50% probability is shown in Fig. S2.† Detailed crystal data and structure refinements are summarized in Table S1.†

Conclusions

For the first time, complete structure elucidation including heavy atoms and atoms of the organic ligands was conducted on black crystalline product $[Au_{11}(PPh_3)_8(C{\equiv}CPh{-}CF_3)_2](SbF_6)$ that was obtained from the reduction of PPh_3AuCl and CF_3-$PhC{\equiv}CAu$ with $NaBH_4$ in methanol. The crystal structure crystallizes in triclinic *P*-1 space group with the same almost C_{3v} symmetric constitution. In the molecular structure, the coordination polyhedron of the gold atoms derived from a centered icosahedron, and unlike in the other gold system two alkynides are exclusively in their μ_1-η1 coordination mode for this undecagold cluster. The Au–Au distances with a mean value of 2.7934 Å are in good agreement with those gold clusters in general. The optical absorbance of a solution of **1** reveals several features that are characteristic of gold cluster molecules. In accordance with the literature, only one singlet in the $^{31}P\{^1H\}$ NMR spectrum is found.

Since the composition of **1** represents a missing link in undecagold cluster chemistry, these findings close this important gap and are considered to promote scientific progress in the understanding of molecular precision synthesis, functionalization of gold nanoparticles and their electronic structure.

Conflicts of interest

There are no conflicts to declare.

Acknowledgements

This work was supported by (a) National Nature Science Foundation of China (No. 22065035 and 21968036), (b) Doctoral Scientific Research Foundation of Yulin university (No. 18GK24), (c) Joint Fund of the Yulin University and the Dalian National Laboratory for Clean Energy (No. 2021007), (d) Social development projects of Shaanxi science and Technology Department (No. 2020SF-408), (e) Project of Shaanxi Provincial Department of Education (No. 20JC039, 21JP148, 21JP146 and 21JS047) and (f) Key R & D projects of Shaanxi Provincial Department of science and technology (No. 2021GY-165).

Notes and references

1 Y. Yin and A. P. Alivisatos, *Nature*, 2005, **437**, 664.
2 P. X. Liu, R. X. Qin, G. Fu and N. F. Zheng, *J. Am. Chem. Soc.*, 2017, **139**, 1228.
3 G. R. Zhang, T. Wolker, D. J. S. Sandbeck, M. Munoz, K. J. J. Mayrhofer, S. Cherevko and B. J. M. Etzold, *ACS Catal.*, 2018, **8**, 8244.
4 H. Shen, Y.-Z. Han, Q. Y. Wu, J. Peng, B. K. Teo and N. F. Zheng, *Small Methods*, 2020, **5**, 2000603.
5 R. Dorel and A. M. Echavarren, *Chem. Rev.*, 2015, **115**, 9028.
6 J. O. Meseguer, J. R. C. Antonino, I. Domínguez, A. L. Pérez and A. Corma, *Science*, 2012, **338**, 1452.
7 P. X. Liu, R. X. Qin, G. Fu and N. F. Zheng, *J. Am. Chem. Soc.*, 2017, **139**, 2122.
8 G. Li and R. C. Jin, *Acc. Chem. Res.*, 2013, **46**, 1749.
9 S. Yamazoe, K. Koyasu and T. Tsukuda, *Acc. Chem. Res.*, 2014, **47**, 816.
10 R. X. Qin, K. L. Liu, Q. Y. Wu and N. F. Zheng, *Chem. Rev.*, 2020, **120**, 11810.
11 K. J. Li, R. X. Qin, K. L. Liu, W. T. Zhou, N. Liu, Y. Z. Zhang, Sh. J. Liu, J. Chen, G. Fu and N. F. Zheng, *ACS Appl. Mater.*, 2021, **13**, 52193.
12 R. Ch. Jin, Ch. J. Zeng, M. Zhou and Y. X. Chen, *Chem. Rev.*, 2016, **116**, 10346.
13 H. Shen, E. Selenius, P. P. Ruan, X. H. Li, P. Yuan, O. Lopez-Estrada, S. Malola, Sh. Ch. Lin, B. K. Teo, H. Häkkinen and N. F. Zheng, *Chem.–Eur. J.*, 2020, **141**, 11905.
14 H. Shen, S. J. Xiang, Zh. Xu, Ch. Liu, X. H. Li, C. F. Sun, Sh. C. Lin, B. K. Teo and N. F. Zheng, *Nano Res.*, 2020, **13**, 1908.
15 A. D. Jewell, H. L. Tierney and E. C. H. Sykes, *Phys. Rev. B: Condens. Matter Mater. Phys.*, 2010, **82**, 205401.
16 C. Vericat, M. E. Vela, G. Benitez, P. Carro and R. C. Salvarezza, *Chem. Soc. Rev.*, 2010, **39**, 1805.
17 P. Maity, S. Takano, S. Yamazoe, T. Wakabayashi and T. Tsukuda, *J. Am. Chem. Soc.*, 2013, **135**, 9450.
18 C. M. Crudden, J. H. Horton, I. I. Ebralidze, O. V. Zenkina, A. B. McLean, B. Drevniok, Z. She, H. B. Kraatz, N. J. Mosey, T. Seki, E. C. Keske, J. D. Leake, A. Rousina-Webb and G. Wu, *Nat. Chem.*, 2014, **6**, 409.
19 H. Al-Johani, E. Abou-Hamad, A. Jedidi, C. M. Widdifield, J. Viger-Gravel, S. S. Sangaru, D. Gajan, D. H. Anjum, S. Ould-Chikh, M. N. Hedhili, A. Gurinov, M. J. Kelly, M. El Eter, L. Cavallo, L. Emsley and J. M. Basset, *Nat. Chem.*, 2017, **9**, 890.
20 Z. Cao, J. S. Derrick, J. Xu, R. Gao, M. Gong, E. M. Nichols, P. T. Smith, X. Liu, X. Wen, C. Coperet and C. J. Chang, *Angew. Chem., Int. Ed.*, 2018, **57**, 4981.
21 F. Q. Zhang, J. J. Fang, L. Huang, W. M. Sun, Z. Lin, Z. Q. Shi, X. W. Kang and S. W. Chen, *ACS Catal.*, 2019, **9**, 98.
22 H. Shen, L. Zh. Wang, O. López-Estrada, Ch. Y. Hu, Q. Y. Wu, D. Cao, S. Malola, B. K. Teo, H. Häkkinen and N. F. Zheng, *Nano Res.*, 2021, **14**, 3303.
23 Y. Du, H. Sheng, D. Astruc and M. Zhu, *Chem. Rev.*, 2020, **120**, 526.
24 L. Naldini, F. Cariati, G. Simonetta and L. Malatesta, *Chem. Commun.*, 1966, **18**, 647.
25 M. McPartlin, R. Mason and L. Malatesta, *J. Chem. Soc. D*, 1969, 334.

26 K. Konishi, in *Gold Clusters, Colloids and Nanoparticles I*, Springer International Publishing: Berlin, 2014, vol. 161, p. 49.

27 H. Shen, E. Selenius, P. P. Ruan, X. H. Li, P. Yuan, O. Lopez-Estrada, S. Malola, Sh. Ch. Lin, B. K. Teo, H. Häkkinen and N. F. Zheng, *Chem.–Eur. J.*, 2020, **141**, 11905.

28 D. M. P. Mingos, Structural and Bonding Issues in Clusters and Nano-Clusters, in *Gold Clusters, Colloids, and Nanoparticles II*, ed., Mingos, D. M. P., Structure and Bonding, Springer International Publishing, Berlin, 2014, vol. 162, p. 1.

29 S. Chen, R. Wojcieszak, F. Dumeignil, E. Marceau and S. Royer, *Chem. Rev.*, 2018, **118**, 11023.

30 X. T. Yuan, S. Malola, G. Ch. Deng, F. J. Chen, H. Häkkinen, B. K Teo, L. S. Zheng and N. F. Zheng, *Inorg. Chem.*, 2021, **60**, 3529.

31 P. Yuan, R. H. Zhang, E. Selenius, P. P. Ruan, Y. R. Yao, Y. Zhou, S. Malola, H. Häkkinen, B. K. Teo, Y. Cao and N. F. Zheng, *Nat. Commun.*, 2020, **11**, 2229.

32 X. K. Wan, J. Q. Wang and Q. M. Wang, *Angew. Chem., Int. Ed.*, 2021, **60**, 20748.

33 G. Schmid, R. Pfeil, R. Boese, F. Bandermann, S. Meyer, G. H. M. Calis and W. A. Vandervelden, *Chem. Ber.*, 1981, **114**, 3634.

34 H. Shen and T. Mizuta, *Chem.–Eur. J.*, 2017, **23**, 17885.

35 M. Qu, H. Li, L. H. Xie, S. T. Yan, J. R. Li, J. H. Wang, C. Y. Wei, Y. W. Wu and X. M. Zhang, *J. Am. Chem. Soc.*, 2017, **139**, 12346.

36 A. K. Gupta and A. Orthaber, *Chem.–Eur. J.*, 2018, **24**, 7536.

37 F. Q. Zhang, J. J. Fang, L. Huang, W. M. Sun, Z. Lin, Z. Q. Shi, X. W. Kang and S. W. Chen, *ACS Catal.*, 2019, **9**, 98.

38 F. Hu, Z. J. Guan, G. Y. Yang, J. Q. Wang, J. J. Li, Sh. F. Yuan, G. J. Liang and Q. M. Wang, *J. Am. Chem. Soc.*, 2021, **143**, 17059.

39 X. L. Pei, Z. J. Guan, Z. A. Nan and Q. M. Wang, *Angew. Chem., Int. Ed.*, 2021, **60**, 14381.

40 P. D. Jadzinsky, G. Calero, C. J. Ackerson, D. A. Bushnell and R. D. Kornberg, *Science*, 2007, **318**, 430.

41 D. E. Jiang, *Nanoscale*, 2013, **5**, 7149.

42 Y. Pei, R. Pal, C. Y. Liu, Y. Gao, Z. H. Zhang and X. C. Zeng, *J. Am. Chem. Soc.*, 2012, **134**, 3015.

43 D. E. Jiang, S. H. Overbury and S. Dai, *J. Am. Chem. Soc.*, 2013, **135**, 8786.

44 Y. Yu, Z. Luo, D. M. Chevrier, D. T. Leong, P. Zhang, D. E. Jiang and J. P. Xie, *J. Am. Chem. Soc.*, 2014, **136**, 1246.

45 X. K. Wan, Q. Tang, S. F. Yuan, D. E. Jiang and Q. M. Wang, *J. Am. Chem. Soc.*, 2015, **137**, 652.

46 X. K. Wan, S. F. Yuan, Q. Tang, D. E. Jiang and Q. M. Wang, *Angew. Chem., Int. Ed.*, 2015, **54**, 5977.

47 X. K. Wan, W. W. Xu, S. F. Yuan, Y. Gao, X. C. Zeng and Q. M. Wang, *Angew. Chem., Int. Ed.*, 2015, **54**, 9683.

48 Y. Wang, H. F. Su, L. T. Ren, S. Malola, S. C. Lin, B. K. Teo, H. Häkkinen and N. F. Zheng, *Angew. Chem., Int. Ed.*, 2016, **55**, 15152.

49 Y. Wang, H. F. Su, C. F. Xu, G. Li, L. Gell, S. C. Lin, Z. C. Tang, H. Häkkinen and N. F. Zheng, *J. Am. Chem. Soc.*, 2015, **137**, 4324.

50 J. L. Zeng, Z. J. Guan, Y. Du, Z. A. Nan, Y. M. Lin and Q. M. Wang, *J. Am. Chem. Soc.*, 2016, **138**, 7848.

51 Y. Wang, X.-K. Wan, L. T. Ren, H. F. Su, G. Li, S. Malola, S. C. Lin, Z. C. Tang, H. Häkkinen, B. K. Teo, Q.-M. Wang and N. F. Zheng, *J. Am. Chem. Soc.*, 2016, **138**, 3278.

52 L. C. McKenzie, T. O. Zaikova and J. E. Hutchison, *J. Am. Chem. Soc.*, 2014, **136**, 13426.

53 Z. Pang, J. Zhang, W. Cao, X. Kong and X. Peng, *Nat. Commun.*, 2019, **10**, 2454.

54 H. Shen, Zh. Xu, M. S. A. Hazer, Q. Y. Wu, J. Peng, R. X. Qin, S. Malola, B. K. Teo, H. Häkkinen and N. F. Zheng, *Angew. Chem., Int. Ed.*, 2021, **60**, 3752.

55 X. K. Wan, Q. Tang, S. F. Yuan, D. E. Jiang and Q. M. Wang, *Angew. Chem., Int. Ed.*, 2015, **127**, 6075.

56 X. K. Wan, S. F. Yuan, Q. Tang, D. E. Jiang and Q. M. Wang, *J. Am. Chem. Soc.*, 2015, **137**, 652.

57 G. K. Wertheim, J. Kwo, B. K. Teo and K. A. Keating, *Solid State Commun.*, 1985, **55**, 357.

58 B. S. Gutrath, U. Englert, Y. Wang and U. Simon, *Eur. J. Inorg. Chem.*, 2013, **12**, 2002.

59 T.-H. Huang, F.-Z. Zhao, Q.-L. Hu, Q. Liu, T.-C. Wu, D. Zheng, T. Y. Kang, L.-C. Gui and J. Chen, *Inorg. Chem.*, 2020, **59**, 16027.

60 C. Pethe, C. Maichle-Mössmer and J. Strähle, *Z. Anorg. Allg. Chem.*, 1998, **624**, 1207.

61 *CrysAlisPro Version 1.171.35.19*, Agilent Technologies Inc. Oxfordshire, OX5 1QU, 2013, UK.

62 G. M. Sheldrick, *Acta Crystallogr. A*, 2015, **71**, 3.

63 G. M. Sheldrick, *Acta Crystallogr. A*, 2008, **64**, 112.

64 O. V. Dolomanov, L. J. Bourhis, R. J. Gildea, J. A. K. Howard and H. Puschmann, *J. Appl. Crystallogr.*, 2009, **42**, 339.

65 C. B. Hubschle, G. M. Sheldrick and B. Dittrich, *J. Appl. Crystallogr.*, 2011, **44**, 1281.